Chapter 5

Assessment of the cooling capacity of plate tectonics and flood volcanism in the evolution of Earth, Mars and Venus

Abstract

Geophysical arguments against plate tectonics in a hotter Earth, based on buoyancy considerations, require an alternative means of cooling the planet from its original hot state to the present situation. Such an alternative could be extensive flood volcanism in a more stagnant-lid like setting. Starting from the notion that all heat output of the Earth is through its surface, we have constructed two parametric models to evaluate the cooling characteristics of these two mechanisms: plate tectonics and basalt extrusion / flood volcanism. Our model results show that for a steadily (exponentially) cooling Earth, plate tectonics is capable of removing all the required heat at a rate of operation comparable to or even lower than its current rate of operation, contrary to earlier speculations. The extrusion mechanism may have been an important cooling agent in the early Earth, but requires global eruption rates two orders of magnitude greater than those of known Phanerozoic flood basalt provinces. This may not be a problem, since geological observations indicate that flood volcanism was both stronger and more ubiquitous in the early Earth. Because of its smaller size, Mars is capable of cooling conductively through its lithosphere at significant rates, and as a result may have cooled without an additional cooling mechanism. Venus, on the other hand, has required the operation of an additional cooling agent for probably every cooling phase of its possibly episodic history, with rates of activity comparable to those of the Earth.

This chapter has been submitted by P. van Thienen, N.J. Vlaar and A.P. van den Berg for publication in *Journal of Geophysical Research*.

5.1 Introduction

The literature of the past decades contains several examples of parameterized convection models for the secular cooling of the Earth during its history (e.g. Sharpe and Peltier, 1978; Davies, 1980; Turcotte, 1980; Spohn and Schubert, 1982; Christensen, 1985; Honda and Iwase, 1996; Yukutake, 2000). Depending on the parameters which are chosen, these models show varying rates of cooling for the Earth. Similar models have been produced for Mars (e.g. Stevenson et al., 1983; Schubert and Spohn, 1990; Nimmo and Stevenson, 2000) and Venus (e.g. Solomatov and Zharkov, 1990; Parmentier and Hess, 1992). These are generally based on a power-law relation between the vigour of convection, represented by the thermal Rayleigh number, and the surface heat flow, represented by the Nusselt number. This latter corresponds to the transport of heat through the boundary between the solid and liquid/gaseous planetary spheres. In the modern Earth, this transport is part of the plate tectonic process, which in fact forms a quite efficient convective cooling mechanism (see Figure 5.1a).

The early Earth, however, is thought to have been hotter by up to several hundreds of

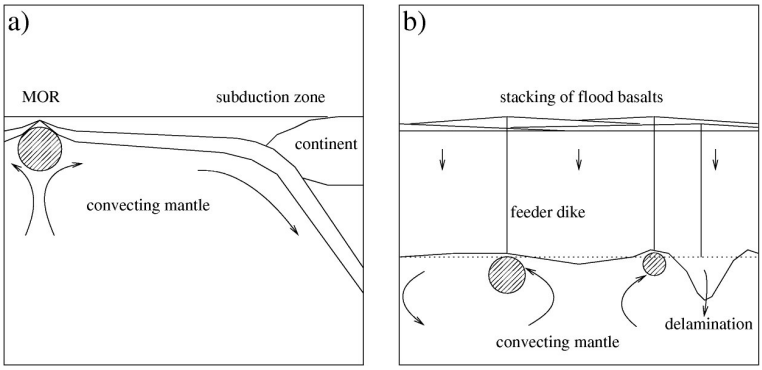

Figure 5.1: Visualization of the plate tectonics and extrusion mechanisms. a) Plate tectonics. A lithospheric column is produced at the mid-ocean ridge by partial melting of upwelling material (hatched area). As it moves towards the subduction zone, it cools down and the lithosphere thickens. At some point, the heat flow through the surface may match the mantle heat flow into the base of the lithosphere, and a steady state situation is reached. b) Extrusion mechanism. Partial melting in the hot convecting mantle mantle underneath the lithosphere (hatched areas) generates basaltic melts that migrate up to the surface, where they form flood basalts. As layer after layer of flood basalts is stacked onto the rest, lower crustal material may delaminate. Essentially the crust itself convects, upwards in the melt phase and downwards in the solid phase. Cooling takes place both by the advection of heat by the basalt and by conduction from the mantle through the lithosphere. The downward convection of the crust will decrease the conductive heat flux out of the mantle.

Kelvin (e.g. Nisbet et al., 1993). In a hotter Earth plate tectonics is counteracted by a thicker layering of oceanic crust and depleted crustal root produced in the melting process, remaining positively buoyant over very long times (Sleep and Windley, 1982), thus preventing subduction to take place (Vlaar, 1986; Vlaar and Van den Berg, 1991; Van Thienen et al., 2003c, chapter 4). Venus and Mars presently do not have plate tectonics (Nimmo and McKenzie, 1996; Zuber, 2001).

The timing of the initiation of modern style plate tectonics is still under debate. Whereas some authors interpret all observations on Archean cratons in a plate-tectonic framework (De Wit, 1998; Kusky, 1998), others find the differences between the Archean granite-greenstone terrains and Phanerozoic tectonically active areas sufficiently large to discount plate tectonics as the mechanism of formation (Hamilton, 1998). The resulting range in estimates for the initiation of plate tectonics is 4.2-2.0 Ga. Ophiolites are considered to be obducted oceanic crust, and are therefore often used as a proxy for plate tectonics (e.g. Kusky et al., 2001). The oldest undisputed ophiolite sequences are about 2 Gyr old. The discovery of a 2.5 Ga ophiolite sequence in China (Kusky et al., 2001) has been disputed by others (Zhai et al., 2002).

An alternative mechanism to plate tectonics for the recycling of oceanic crust into the mantle may be the formation of eclogite in the deep lower parts of a thickened basaltic crust, which subsequently delaminates due to its intrinsic higher density. This process was modeled by Vlaar et al. (1994). The upward transport of melts to produce a basaltic crust and the downward movement of earlier layers of basalt below this, together with delaminating eclogite, in fact form a small scale convection cycle in the lithosphere itself (see Figure 5.1b). The delamination of eclogite allows the upward flow of fertile material that can then melt and add more basalt to the crust. This in theory is a very efficient way of removing heat from the Earth. Furthermore, it is consistent with geological evidence, which indicates that flood volcanism was quite common during the Archean (Arndt, 1999).

In this work we will evaluate the potential effect of both cooling mechanisms on the cooling history of the Earth, Mars and Venus. Reese et al. (1998) have also investigated the cooling efficiency of plate tectonics and stagnant lid regimes on Earth, Mars and Venus, using both boundary layer analysis and numerical models. However, here we apply a different approach to both modelling the cooling behaviour and examining the parameter space in which all plausible cooling histories of the terrestrial planets are defined.

In our models, the amount of activity required to obtain a certain cooling rate is determined as a function of potential temperature. More specifically, in the case of plate tectonics, we determine how fast it must operate to generate a certain planetary mantle cooling rate. We express this rate of operation with a parameter called the turnover time τ, which indicates the average lifetime of oceanic lithosphere from creation at a mid-ocean ridge to its removal from the planetary surface and return into the mantle at a subduction zone. In the case of flood volcanism, we ascertain the average volumetric rate of basalt production, expressed as an equivalent layer thickness added to the global surface area (or an active fraction of this) per unit time: the extrusion rate δ.

As the exact cooling history of the terrestrial planets remains unknown, we construct several model cooling histories that are then evaluated in the framework of the two cooling mechanisms described above. This allows us to estimate the rates of activity of the mech-

anisms in the early planetary histories, which for the Earth can be linked to geological observations.

5.2 Numerical model

For the two different geodynamical regimes described above we apply two different numerical models. The first, concerning the plate tectonics regime, is presented in section 5.2.1. The second, which concerns the basalt extrusion mechanism, will be treated in section 5.2.2.

The basic heat balance equation is applied:

$$C\frac{d}{dt} < T >= H_T - Q \tag{5.1}$$

with

$$C = \int_V \rho c_p dV \tag{5.2}$$

$$H_T = \int_V H dV \tag{5.3}$$

$$Q = \int_{\delta V} \vec{q} \cdot \vec{n} dA = Q_{surf} - Q_{core} \tag{5.4}$$

The symbols are explained in Table 5.1. The heat fluxes through the top and bottom boundaries of the model are combined in the term Q of equation (5.4). The Q_{surf}-term is different for the two mechanisms that are studied. The definition of this term for each mechanism will be given below. The total heat flux out of the mantle is treated separately in the following sections. The core heat flux into the mantle is used as an input parameter, and the choice of its value will be discussed below in section 5.2.3. The internal heating due to the decay of radioactive elements is represented by H_T in equation (5.3).

symbol	parameter	definition	value/unit
A	surface area		m^2
C	mantle heat capacity		JK^{-1}
c_p	specific heat		$\mathrm{Jkg}^{-1}\mathrm{K}^{-1}$
d_{lith}	lithosphere thickness		m
f	active fraction of surface area		-
k	thermal conductivity	$\kappa\rho c_p$	$\mathrm{Wm}^{-1}\mathrm{K}^{-1}$
H	radiogenic heating rate		Wm^{-3}
H_T	mantle radiogenic heating rate		W
N	number of oceanic ridges		-
$\vec{n}$	normal vector		-
n	order of plate model series		-
Q	heat flux		W
Q_{core}	core heat flux		W
Q_{surf}	surface heat flux		W
$\vec{q}$	heat flow	$-k\nabla T$	Wm^{-2}
q_0	surface heat flow	$-k\frac{dT}{dz}$	Wm^{-2}
R	planetary radius		km
R_{core}	core radius		km
T	temperature		$^{\mathrm{o}}\mathrm{C}$
T_{pot}	potential temperature		$^{\mathrm{o}}\mathrm{C}$
T_{surf}	surface temperature		$^{\mathrm{o}}\mathrm{C}$
t	time/age		s
u	half spreading rate		ms^{-1}
$\vec{u}$	velocity		ms^{-1}
V	volume		m^3
w	vertical velocity		ms^{-1}
y_{L0}	plate thickness		m
δ	extrusion rate		ms^{-1}
θ	latitude		radians
κ	thermal diffusivity		$\mathrm{m}^2\mathrm{s}^{-1}$
ρ	density		kgm^{-3}
τ	turnover time		s
ϕ	angle / longitude		radians

Table 5.1: Symbol definitions

Although equation (5.1) describes the rate of change of the volume averaged temperature of the mantle, we want to express the results in terms of potential mantle temperature. Therefore we have obtained a simple relation between the rates of change of the volume averaged and potential temperatures. This relation was determined by volume integration in a spherical shell of several synthetic geotherms (adiabatic profile at depth and

linear profile in top 100 km). The resulting expression, showing excellent correlation ($R > 0.999$), is:

$$\frac{d}{dt} < T >= f_{T_{avg}} \frac{d}{dt} T_{pot} \tag{5.5}$$

The scaling factor $f_{T_{avg}}$ is different for the different planets because of size effects. The values are listed in Table 5.2.

property	Earth	Mars	Venus
R (km)	6371	3397	6052
R_{core} (km)	3480	$1700^{(1),(2),(3)}$	$3400^{(4)}$
$c_{p_m}(\mathrm{Jkg^{-1}K^{-1}})$	$1250^{(5)}$	$1250^{(5)}$	$1250^{(5)}$
$g_0(\mathrm{ms^{-2}})$	$9.81^{(6)}$	$3.7^{(6)}$	$8.9^{(6)}$
$T_{surf}(^{\mathrm{o}}\mathrm{C})$	$15^{(6)}$	$-55^{(6)}$	$457^{(6)}$
$M(\mathrm{kg})$		$6.42 \cdot 10^{23\ (6)}$	
M_{sm}/M		$0.75^{(2)}$	
$< \rho_m > (\mathrm{kgm^{-3}})$	$4462^{(6)}$	3350	$4234^{(4)}$
$Q_{core}(\mathrm{TW})$	$3.5 - 10^{(7),(8)}$	$0.4^{(9)}$	0
$f_{T_{avg}}$	1.30	0.997	1.23

Table 5.2: Values for the planetary radius R, core radius R_{core}, average mantle specific heat c_{p_m}, gravitational acceleration g_0, surface temperature T_{surf}, planetary mass M, relative silicate mantle mass M_{sm}/M, average mantle density $< \rho_m >$, core heat flux Q_{core} and temperature scaling term $f_{T_{avg}}$ (see text) used in the calculations for Earth, Mars and Venus. The average mantle density for Mars is calculated using planetary mass, silicate mantle mass fraction, and planetary and core size. References are: (1) Folkner et al. (1997), (2) Sanloup et al. (1999), (3) Yoder et al. (2003), (4) Zhang and Zhang (1995), (5) based on data from Saxena (1996) and Stixrude and Cohen (1993), (6) Turcotte and Schubert (2002), (7) Sleep (1990), (8) Anderson (2002), (9) heat flow from Nimmo and Stevenson (2000) for a 1700 km core.

To simplify the formulation of the problem, we assume that all heat transport from the mantle to the surface takes place in oceanic environments for plate tectonics. This is justified for the Earth by computing the magnitude of the continental mantle heat flow: Eighty-six percent of the present continental heat flux is accounted for by radiogenic heating, 58 percent of which is generated in the continental crust itself (Vacquier, 1998). Since about 30 percent of the global heat flux is through continental areas (Sclater et al., 1980; Pollack et al., 1993), this means that 15 percent of the current global heat flux is mantle heat (both radiogenic heat from the mantle and heat from mantle cooling) flowing through continental areas. We expect this fraction to be significantly smaller for the earlier Earth, because of the higher radiogenic heat production (causing a stronger blanketing effect) accompanied by a smaller amount of continental area relative to the oceanic domain. Furthermore, thicker roots of Archean cratons compared to post-Archean continental roots may divert mantle heat from the cratons (Davies, 1979; Ballard and Pollack, 1987, 1988).

For the extrusion models, we assume activity over the entire surface of the planets, since extensive volcanism on Earth also occurs in both continental (flood volcanism) and oceanic (plateaus) environments. Because both Venus and Mars do not have clearly distinguishable oceanic and continental areas, no continents will be taken into account for these planets.

5.2.1 Plate tectonics

In order to obtain an expression for the global surface heat flux Q_{surf} for the plate tectonics model, we use a plate model approximation (Carslaw and Jaeger, 1959; McKenzie, 1967; Turcotte and Schubert, 2002). The surface heat flow for this plate model is given by the following equation:

$$q_0(t) = \frac{k(T_1 - T_0)}{y_{L0}} \left[1 + 2 \sum_{n=1}^{\infty} \exp\left(-\frac{\kappa n^2 \pi^2 t}{y_{L0}^2} \right) \right] \tag{5.6}$$

In this equation, q_0 is the surface heat flow, k the thermal conductivity, T_0 and T_1 the surface and basal plate temperatures, y_{L0} the plate thickness, κ the thermal diffusivity and $t = x/u_0$ the age of the lithosphere, see Table 5.1, where x is the distance to the spreading ridge and u_0 the constant half spreading velocity.

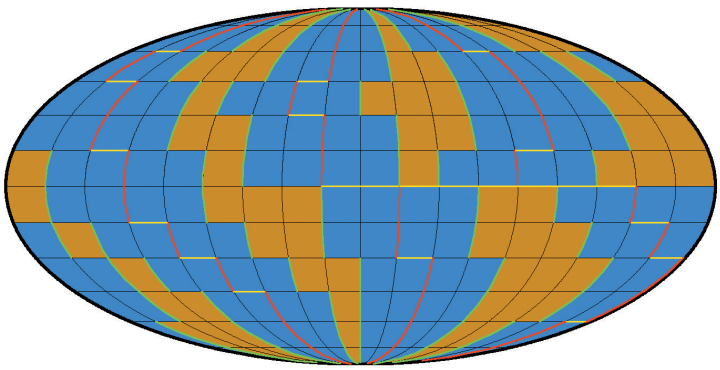

Figure 5.2: Conceptual visualization of the parameterization of plate tectonics as described in section 5.2.1 in a Mollweide projection, for a situation in which three oceans ($N = 3$) cover two thirds of the Earth's surface area. All oceans (blue) have the same uniform longitudinal extent ϕ, are bounded by subduction zones (green) at active continental (brown) margins, and have mid-ocean ridges (red) in the middle. Transform faults (yellow) may offset the ridge and consequently also the margin of the oceans. Note that only the transform faults connecting parts of ridge axes have been drawn.

In order to obtain the global surface heat flux, we need to integrate this equation over the entire planet's oceanic surface, and to do this we make some assumptions on the geometry of the system.

We consider a spherical planet that is divided in pole to pole segments. These are separated by subduction zones and continents and each has a central spreading ridge. The boundaries and ridges may be offset by transform faults, which will not influence the argumentation (see Figure 5.2). If such a segment has a longitudinal extent ϕ, its surface area A_s equals

$$A_s = 2\phi R^2 \tag{5.7}$$

We define the average time required to renew all oceanic crust as the turnover time τ. If we assume a fraction f of the entire planet's surface to be oceanic, i.e. involved in the plate tectonics system, divided in N segments of equal size, we can compute the turnover time τ by dividing the active surface area by the time derivative of the segment surface area:

$$\tau = \frac{4\pi R^2 f}{\frac{dAs}{dt}} = \frac{4\pi R^2 f}{2NR^2\frac{d\phi}{dt}} = \frac{2\pi f}{N\frac{d\phi}{dt}} \tag{5.8}$$

which gives us

$$\frac{d\phi}{dt} = \frac{2\pi f}{N\tau} \tag{5.9}$$

In this framework, the lithospheric age t in equation (5.6) can be rewritten:

$$t = \frac{x}{u} = \frac{\phi R cos\theta}{\frac{1}{2}\frac{d\phi}{dt}Rcos\theta} = \frac{\phi}{\frac{1}{2}\frac{d\phi}{dt}} \tag{5.10}$$

with x the distance from the ridge, ϕ the corresponding longitudinal extent, θ the latitude and u the half spreading rate (hence the factor $\frac{1}{2}$ in the denominator of this expression).

We now compute the global oceanic heat flux by integrating equation (5.6) over the entire oceanic surface. This is done by considering $2N$ sections of oceanic crust from ridge to subduction zone, that have a longitudinal extent of

$$\phi_n = \frac{1}{2}\cdot\frac{2\pi f}{N} \tag{5.11}$$

The global oceanic heat flux now becomes

$$Q_{surf} = 2N\int_{\phi=0}^{\frac{\pi f}{N}}\int_{\theta=0}^{\pi}\frac{k\Delta T}{y_{L0}}\cdot$$

$$\left[1 + 2\sum_{n=1}^{\infty}\exp\left(-\frac{\kappa n^2\pi^2}{y_{L0}^2}\cdot\frac{\phi}{\frac{1}{2}\frac{d\phi}{dt}}\right)\right]R^2\sin\theta d\theta d\phi \tag{5.12}$$

Inserting equation (5.9) and integrating over θ gives

$$Q_{surf} = 2N \int_{\phi=0}^{\frac{\pi f}{N}} \frac{2k\Delta T R^2}{y_{L0}} \left[1 + 2\sum_{n=1}^{\infty} \exp\left(-\frac{n^2 \pi \kappa N \tau \phi}{y_{L0}^2 f}\right)\right] d\phi$$

$$= \frac{4k\Delta T R^2 \pi f}{y_{L0}} \left\{1 + 2\sum_{n=1}^{\infty} \frac{y_{L0}^2}{\pi^2 n^2 \tau \kappa} \left[1 - \exp\left(-\frac{n^2 \kappa \tau \pi^2}{y_{L0}^2}\right)\right]\right\} \tag{5.13}$$

Note that the number of ridges N has disappeared from the equation, although Q_{surf} depends on the number of segments N implicitly through τ. As equation (5.8) shows, τ can be constant when simultaneously changing both N and $\frac{d\phi}{dt}$ keeping $N\frac{d\phi}{dt}$ constant. In other words, a smaller number of ridges requires a higher spreading rate to obtain the same turnover time. Although the applied geometry only allows for integer values of N, we will allow it to have non-integer values as well, allowing a continuous range of possible global ridge lengths.

5.2.2 Extrusion mechanism

In the extrusion mechanism, we assume that, on long-term average, material is erupted and spreads out over the entire planetary surface. We define the rate at which this takes place as the extrusion rate δ, which indicates the time derivative of the extruded volume divided by the planetary surface area, or in other words the production of an equivalent thickness of crust per unit time. As all material that is extruded is stacked on top of existing crust in our model, pre-existing crustal material moves downward relative to the surface at the same rate as material is extruded, comparable to the permeable boundary approach of Monnereau and Dubuffet (2002) applied to Io. When (crustal) material reaches the depth of the lithosphere thickness, defined below in section 5.2.3, we assume it to delaminate (see Figure 5.1b). For the extrusion mechanism, a different formulation is used for the surface heat flux term of equation (5.1) than for the plate tectonics model. The surface heat flux Q_{surf} consists of two parts. The first is the heat advected by magma that is extruded onto the surface. We assume the magma to lose all its internal excess heat to the hydrosphere/atmosphere, taking on the surface temperature. The heat flux from this component is described by:

$$Q_{extru} = 4\pi R^2 f \delta \rho c_p \delta T \tag{5.14}$$

In this expression, f is the fraction of the planetary surface on which the mechanism is active, δ is the extrusion rate, and ρ is the density of the solidified magma (see Tables 5.1 and 5.2). δT is the temperature drop of the magma from the potential temperature to the surface temperature. This means that both latent heat consumption upon partial melting and release of latent heat during solidification, which are expected to cancel out, are not included explicitly. The second component of the surface heat flux is the conductive heat flux out of the mantle. Because in this scenario, there is continuous stacking of successive extrusive units, crustal material is continuously pushed downwards. As we assume a

constant lithosphere thickness (for a fixed potential temperature) and a fixed temperature at the lower boundary of the lithosphere consistent with the potential temperature, this causes an increase in the geothermal gradient in the deep lithosphere and a decrease at shallow levels (see Figure 5.3). In order to quantify this, we use a 1-D finite difference model of the thermal state of the lithosphere. We consider the heat equation:

$$\rho c_p \left(\frac{\partial T}{\partial t} + \vec{u} \cdot \nabla T \right) = \partial_j (k \partial_j T) + H \tag{5.15}$$

Steady state geotherms are assumed, and we simplify the equation to one dimension:

$$\rho c_p w \frac{\partial T}{\partial z} = \frac{\partial}{\partial z} \left(k \frac{\partial T}{\partial z} \right) + H \tag{5.16}$$

In this equation the extrusion of basalt is represented by the vertical velocity w, which we define to be equal in magnitude to the extrusion rate δ. We solve this equation numerically for the lithosphere, defined below in section 5.2.3, with the surface temperature and the potential temperature extrapolated to the base of the lithosphere as boundary conditions. A finite difference scheme (using 400 nodes for the lithosphere) is used to obtain geotherm and from this the conductive heat flux at the top of the lithosphere Q_{bl}, out of the mantle (see Figure 5.3).

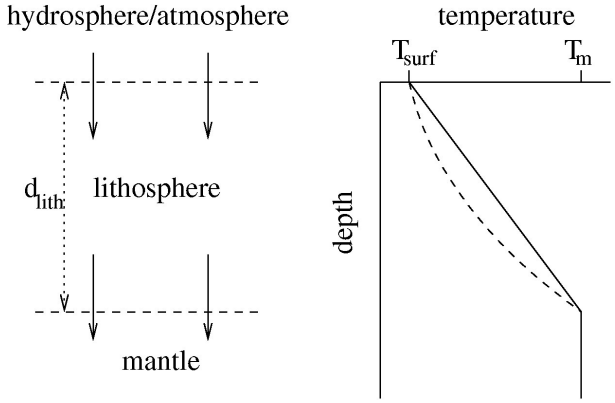

Figure 5.3: 'Lithospheric convection' in which, at the top boundary, material is added by magma extrusion and at the bottom boundary material is lost due to delamination, resulting in a constant lithosphere thickness. Geotherms are computed for this setting using expression (5.16) in a finite difference scheme, see text. For a situation without radiogenic heating, the trivial case of $w = \delta = 0$ (no extrusion and delamination) results in a linear geotherm (solid curve). For a finite downward velocity, the geotherm is deflected (dashed curve), resulting in a decreased conductive heat flux through the lithosphere.

Together the two components form the total surface heat flux:

$$Q_{surf} = Q_{extru} + Q_{bl} \tag{5.17}$$

5.2.3 Input parameters

The main input parameters for the different planets are listed in Table 5.2. The least constrained parameter in the models is the heat flux from the core into the mantle. Recent estimates for the present-day Earth range from 2.0 TW to 12 TW (Sleep, 1990; Anderson, 2002; Buffett, 2003). The former estimate is based on hotspot fluxes interpreted as associated with mantle plumes originating at the core mantle boundary (CMB) and, as Labrosse (2002) argues, is probably a lower limit because not all plumes that start at the CMB would make it to the surface. The latter is based on an evaluation of mantle heat transfer mechanisms near the CMB (Anderson, 2002; Buffett, 2003). Estimates for the core heat flux during the (early) history of the Earth are even more difficult to make. Thermal evolution calculations by Yukutake (2000) show the core heat flux decreasing from 12 TW at 4.4 Ga to a present value of 7.5 TW. A decreasing value is also found in the models of Labrosse et al. (1997). Buffett (2003) calculated that in the early Earth, before the formation of an inner core (the timing of which is uncertain, but in the range of 1.9-3.2 Ga, Yukutake, 2000), a core heat flux of about 15 TW would be required to drive the geodynamo. However, an increase of the core heat flux during the history of the Earth also seems plausible. Large temperature contrasts over the D" layer (δT about 1200 K, Anderson, 2002) have been inferred suggesting slow heat transfer from the core. Recent results of numerical mantle convection modelling including temperature and pressure dependent thermal conductivity show a core heat flux fluctuating around a slightly increasing value and a temperature contrast across the bottom boundary layer increasing with time, showing the mantle to cool faster than the core, in line with planetary cooling from the top down (Van den Berg et al., 2003).

It is even more difficult to estimate the core heat fluxes for Mars and Venus. Nimmo and Stevenson (2000) reasoned that, as a superadiabatic temperature gradient is required to drive convection, the maximum obtainable conductive heat flow would be realised along an adiabatic thermal gradient. They estimated this number for the Martian core to be $5 - 19 mW m^{-2}$. The absence of a magnetic field suggests that the martian core does not convect and therefore this number may be an upper limit for the current martian core heat flow. Using a value of $10 mW m^{-2}$ and a core radius of 1700 km (see Table 5.2), this results in a core heat flux of 0.4 TW. For Venus, the adiabatic conductive heat flow would be $11 - 30 mW m^{-2}$ (Nimmo, 2002). However, the calculations of Turcotte (1995) and Nimmo (2002) indicate that the mantle of Venus may be heating up and the core heat flux would therefore be declining. We will therefore not consider a core heat flux for Venus in our calculations.

Other input parameters that are not well constrained are the thickness of the cooling plate (in the plate model, used in the plate tectonics formulation, see section 5.2.1) and the lithosphere (used in the extrusion model, see section 5.2.2) as a function of potential temperature. The plate thickness does not directly correspond to a physical thickness of

crust or lithosphere, but is obtained by matching the plate model heat flow with oceanic heat flow measurements. The (thermal) lithospheric thickness is defined by the 1327^oC (1600 K) isotherm (Turcotte and Schubert, 2002). Since the rheology of mantle material is strongly temperature dependent (e.g. Karato and Wu, 1993), the thickness of the (rheological) lithosphere is a function of the potential mantle temperature. We have obtained a parameterization for both the plate thickness in the plate tectonics model and the lithospheric thickness in the extrusion model using 2-D numerical convection models. A finite element mantle convection code (see Van den Berg et al., 1993) was used in these experiments. The experimental setup for the plate tectonics model is indicated in Figure 5.4a. Upwelling is prescribed in the left hand side limb of the model domain. A nonzero velocity corresponding to the plate velocity is prescribed on (most of) the top boundary. A relatively low half spreading rate of about 4 mm/yr is used to limit the length of lithosphere required to reach thermal equilibrium. Material leaves the domain through the right hand side boundary with the prescribed plate velocity. The lower boundary of the long horizontal limb of the domain is open and kept at a temperature consistent with the potential temperature of the model, allowing relatively warm material to rise into the domain and cold material to sink out of the domain. The viscosity is temperature and pressure dependent, using parameters from Karato and Wu (1993) halfway between their wet and dry parameters. We determined the surface heat flow for the steady state part of the lithosphere (far from the ridge, see Figure 5.4b). Through trial-and-error, we searched for an effective plate thickness y_{L0} in equation (5.6) to match the heat flow at the potential temperature of each model characterized by the value of the potential temperature T_{pot}. Because the models are kinematically driven, buoyancy is of minor importance and the results are insensitive to gravitational acceleration and therefore applicable to Mars and Venus as well. Second-order motion in the form of small-scale sublithospheric convection (see Parsons and Sclater, 1977; Sleep, 2002) may be different on the different planets due to possible differences in gravitational acceleration and mantle viscosity. As a consequence of the different gravity, the Rayleigh number describing this process will be a factor 2.5 smaller for Mars than for Earth (since $g_0^{Mars} \approx 0.4 \cdot g_0^{Earth}$), the effect of which is relatively minor. The Rayleigh number scales inversely with mantle viscosity, which may therefore be of greater importance. However, the mantle viscosities of Mars and Venus are not well constrained, but may be higher due to a possibly lower water content, which would cause a greater effective plate thickness. We assume the effective plate thickness parameterization obtained for Earth-like parameters to be valid for Mars and Venus as well, keeping this caveat in mind. The resulting expression for the effective plate thickness y_{L0} is

$$y_{L0} = 147.4 - 0.1453T_{pot} + 2.077 \cdot 10^{-4}T_{pot}^2 - 8.333 \cdot 10^{-8}T_{pot}^3 \tag{5.18}$$

with y_{L0} in km and T_{pot} in degrees Celsius. This expression gives an effective plate thickness of just under 125 km for the present day potential temperature of 1350^oC. This is consistent with results of Parsons and Sclater (1977), but somewhat thicker than the 100 km found by Stein and Stein (1992).

An effective lithospheric thickness for the extrusion models was found using numerical convection simulations in a different, stagnant-lid convection mode. Heating is only

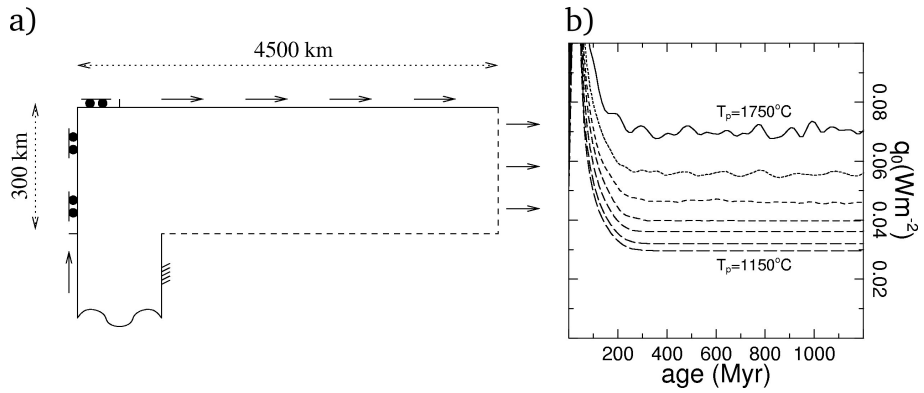

Figure 5.4: a) Numerical model setup. Adiabatic upwelling is prescribed in the left hand side limb of the model domain. A nonzero velocity is prescribed on (most of) the top boundary, corresponding to the plate velocity. Material leaves the domain through the right hand side boundary. The lower boundary of the long horizontal limb of the domain is open and kept at a temperature consistent with the potential temperature of the model. The viscosity is temperature and pressure dependent, using parameters from Karato and Wu (1993). b) Resulting surface heat flows for potential temperature of 1150^oC (long-dashed curve) up to 1750^oC (solid curve) in steps of 100^oC. For these surface heat flows and potential temperatures, a plate thickness was sought that reproduces the surface heat flow in thermal equilibrium (far from the spreading ridge).

internal (zero bottom heat flux), and a zero temperature is prescribed on the top boundary. Side boundaries are periodic. The domain has a depth of 670 km, an aspect ratio of 1.5, a no-slip top boundary and a free slip bottom boundary. A series of models with different internal heating rates was started to generate a range of statistical steady state potential temperatures and lithospheric thicknesses. For each model, the lithospheric thickness, represented by the depth of the 1327^oC isotherm is plotted against the potential temperature and a fit is computed for the entire set (see Figure 5.5):

$$d_{lith} = 6684 - 9.7352 \cdot T_{pot} + 4.7675 \cdot 10^{-3} \cdot T_{pot}^2 - 7.8049 \cdot 10^{-7} \cdot T_{pot}^3 \quad (5.19)$$

with d_{lith} in km and the potential temperature T_{pot} in degrees Celsius. Since these models are not kinematically driven but are convecting actively, we have done the experiments for different values for the gravitational acceleration, representing the different planets (see Table 5.2). As can be seen in Figure 5.5, the results of the experiments described above applied to Mars and Venus (in which the gravitational acceleration is the control parameter) nearly coincide with the best fit curve for Earth, so this curve is used for all planets (the possibly higher mantle viscosities for Venus and Mars, which would cause an increase in the lithosphere thickness, are kept in mind). We have tested the sensitivity of this result to the depth of the domain, rerunning several experiments with a doubled

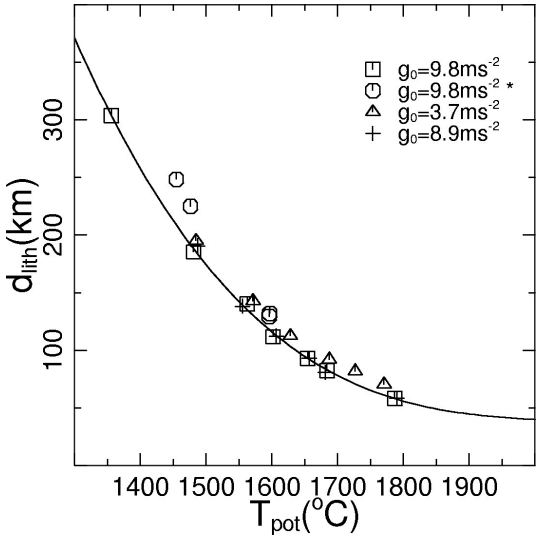

Figure 5.5: Lithosphere thickness as a function of mantle potential temperature in a stagnant lid setting, obtained from numerical convection experiments (see text). Symbols represent experiments for Earth (squares), Earth with a larger model domain (circles, see text), Mars (triangles) and Venus (crosses) values of gravity. The cubic best fit of the Earth data, used in the extrusion models (equation (5.19)), is indicated by the solid curve.

width and depth. Resulting lithosphere thicknesses are slightly greater but of comparable magnitude (see Figure 5.5).

We investigate the sensitivity of the results to the plate and lithosphere thickness, the core heat flux, the internal heating rate and the oceanic surface fraction in sections 5.3.3 and 5.3.7. In a more general planetary context we also investigate the effect of gravitational acceleration, planet size and surface temperature in sections 5.3.5 and 5.3.9.

The average mantle densities for Earth and Mars are calculated by dividing mantle mass over volume. In the case of Venus, we use the average of the results of two four-zone hydrostatic models by Zhang and Zhang (1995). The average heat capacities of the planetary mantles are approximated. Using data from Fei et al. (1991), one can calculate that the Earth's upper mantle heat capacity (for peridotite) is about $1250 Jkg^{-1}K^{-1}$. For the lower, mantle, assuming a two phase assemblage of perovskite and magnesiowüstite, the heat capacity of the assemblage, using data from either Stixrude and Cohen (1993) or Saxena (1996), falls in the range of $1200-1300 Jkg^{-1}K^{-1}$. We therefore apply a uniform value of $1250 Jkg^{-1}K^{-1}$ for the entire Earth's mantle. Because of similar composition and temperatures and a smaller pressure interval in Mars and Venus, the same value is assumed for these planets.

5.2.4 Solving the equation

In the plate tectonics scenario, we solve equation (5.1) for the turnover time τ using equation (5.13) for the surface heat flux. This means we obtain the turnover time that is required to facilitate a specified cooling rate at a specified potential temperature.

In the extrusion mechanism case, we solve equation (5.1) for the extrusion rate δ, using equations (5.14) and (5.17) to obtain the corresponding surface heat flux, which gives us the required extrusion rate to obtain the specified cooling rate at the specified potential temperature.

In both cases, the parameter we want to solve for is not easily isolated from the equations. We therefore apply a bisection algorithm to compute the desired solutions numerically (see Table 5.3).

step	action
0	prescribe potential temperature and cooling rate for this experiment
	prescribe lower and upper boundary for ξ ($\xi_{lb}^{(0)}$ and $\xi_{ub}^{(0)}$) spanning the range in which the value of ξ is expected
	start loop with iteration counter n=1
1	compute $\xi_{bis}^{(n)} = (\xi_{lb}^{(n-1)} + \xi_{ub}^{(n-1)})/2$
2	compute $dT_{pot}/dt\|_{bis} = dT_{pot}/dt(\xi_{bis}^{(n)})$
3	compare $dT_{pot}/dt\|_{bis}$ to prescribed dT_{pot}/dt
	if relative mismatch $< \varepsilon_{bis}$, $\xi = \xi_{bis}^{(n)}$ and loop ends
4	- if $dT_{pot}/dt\|_{bis} < dT_{pot}/dt$, ξ must be greater than $\xi_{bis}^{(n)}$
	$\rightarrow$ increase lower boundary of search domain: $\xi_{lb}^{(n+1)} = \xi_{bis}^{(n)}$
	- if $dT_{pot}/dt\|_{bis} > dT_{pot}/dt$, ξ must be less than $\xi_{bis}^{(n)}$
	$\rightarrow$ decrease upper boundary of search domain: $\xi_{ub}^{(n+1)} = \xi_{bis}^{(n)}$
5	$n = n + 1$ and return to step 1

Table 5.3: Numerical scheme which is used for solving the volume averaged heat equation (5.1), either for the plate tectonics model, in which case ξ indicates the turnover time τ, or for the flood volcanism case, where ξ indicates the extrusion rate δ.

5.3 Results

5.3.1 Mantle cooling rates

Results obtained from the models described in the previous sections are presented below. These results quantify the characteristics of the two cooling mechanisms, plate tectonics and flood volcanism, for specific cooling histories. Since the applied models represent quasi steady states, they do not tell us anything about the cooling histories of the Earth, Mars and Venus themselves. In this section we first explore the range of plausible cooling

histories in $T_{pot}, dT_{pot}/dt$-space, using simple approximations of two types of expected cooling behaviour. These scenarios will then be included in (the discussion of) the figures presenting the results of the model calculations as described in the previous sections, and aid the discussion of the results that may be relevant for the cooling histories of the terrestrial planets. Long-term decaying secular cooling will be approximated by an exponential cooling curve. Short-term cooling pulses will be viewed separately. Figure 5.6 shows five cooling histories in which a simple exponential cooling is assumed from a starting temperature of $1500 - 1900^oC$ at 4.0 Ga to the Earth's present estimated potential temperature of 1350^oC. They were constructed by fitting the start and end points to the expression

$$T = T_0 \exp(at) \tag{5.20}$$

for which the corresponding cooling rate is

$$\frac{dT}{dt} = aT_0 \exp(at) \tag{5.21}$$

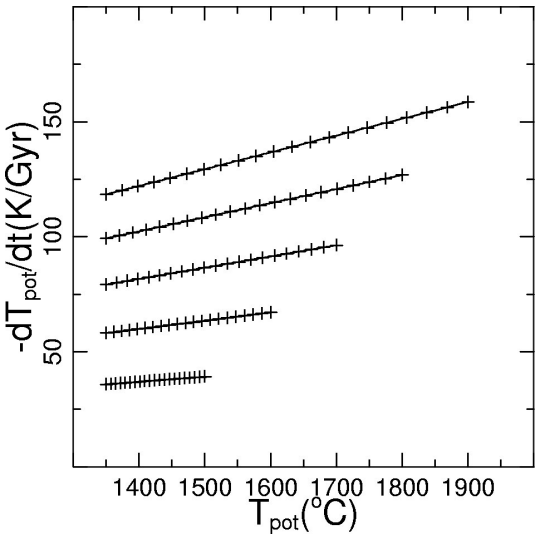

Figure 5.6: Exponential cooling curves in $T_{pot}, dT_{pot}/dt$-space, for starting temperatures of 1500, 1600, 1700, 1800 and 1900^oC. Markers are 200 Myr apart.

Markers are included at 200 Myr intervals to indicate the flow of time. These model cooling histories through $T_{pot}, dT/dt$-space will be used below in the discussion of the results as reference models. The initial temperatures shown seem to cover the range of temperatures inferred for the early Archean Earth mantle, and thus the area spanned by these curves contains plausible cooling histories for a steadily cooling Earth with an

exponential decay of both the potential temperature and the cooling rate. Because of the assumed similar formation histories and sizes of Mars and Venus compared to the Earth, we assume the same mantle temperature window to be valid for these two planets.

However, if the cooling of the planets is not an exponentially decaying process, or if the system diverges from this behaviour from time to time as in an episodic scenario, cooling rates may be significantly higher than those shown in Figure 5.6. This is illustrated by numerical models of secular cooling of the Earth by Van den Berg and Yuen (2002), which show fluctuating cooling rates with peak values of 300 to 500 K/Gyr during the early histories of their experiments. In Figure 5.7, we show maximum cooling rates that are obtained for a Gaussian shaped pulse in the cooling rate (Figure 5.7a,b). Figure 5.7c shows the temperature drop of the mantle caused by this cooling pulse on the horizontal axis. On the vertical axis, the duration of the cooling pulse ($\pm 2\sigma$) is indicated. Obviously high cooling rates are expected for short pulses with a large temperature drop, and lower cooling rates for longer pulses with smaller temperature drops. Nearly everywhere in this figure, the cooling rates are significantly higher than in the steady exponential cooling of Figure 5.6.

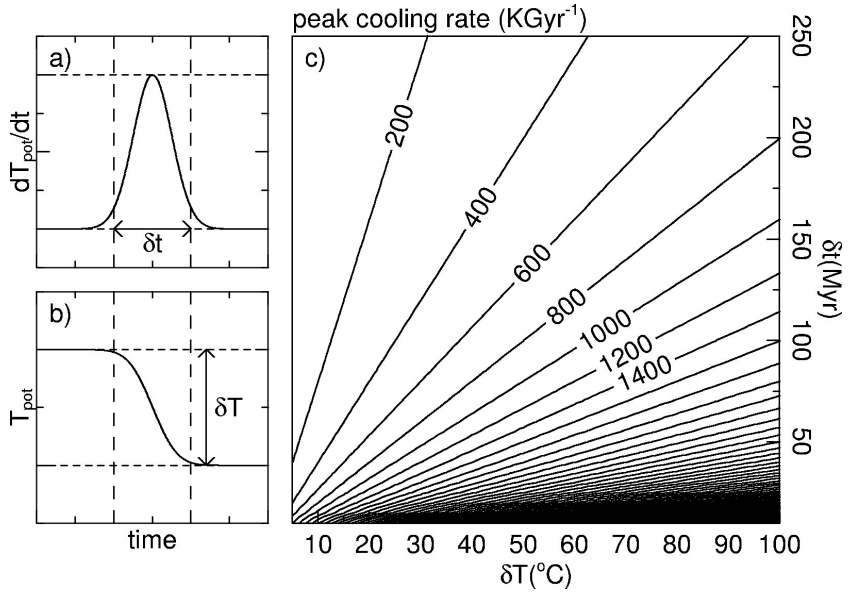

Figure 5.7: Peak cooling rates for mantle cooling pulses with Gaussian shape using arbitrary units (left hand side frames). The corresponding temperature drop is indicated on the horizontal axis, and the vertical axis signifies the duration ($\pm 2\sigma$) of the cooling pulse.

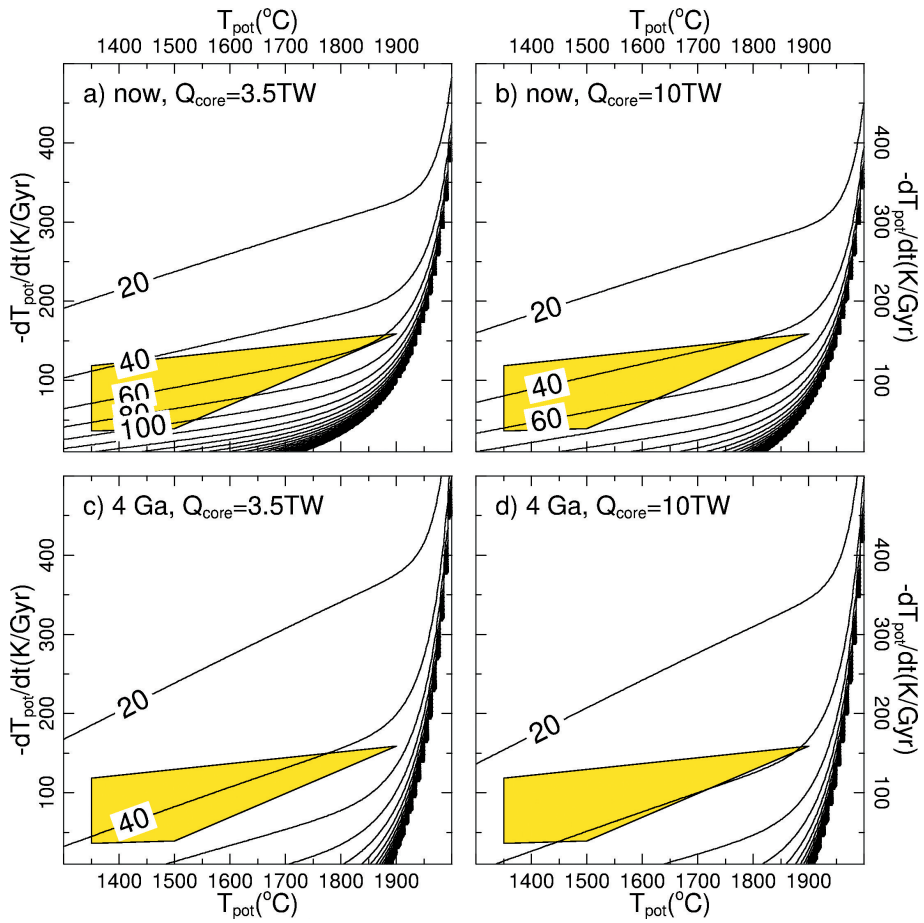

Figure 5.8: Results of the plate tectonics model for a core heat fluxes of 3.5 and 10 TW for the present and early Earth (in terms of radiogenic heat production rate and extent of the continents). Contours indicate the turnover time τ (in Myr) as a function of potential temperature (horizontal axis) and cooling rate (vertical axis). The shaded zone corresponds to the region spanned by the exponential cooling curves of Figure 5.6, and are thus representative of steady state secular cooling. Higher values on the vertical axis may be caused by cooling pulses, see Figure 5.7.

5.3.2 Plate tectonics on Earth

The computed results for the plate tectonics model described in section 5.2.1 applied to the Earth are presented in Figure 5.8a-d, showing contour levels of the turnover time τ,

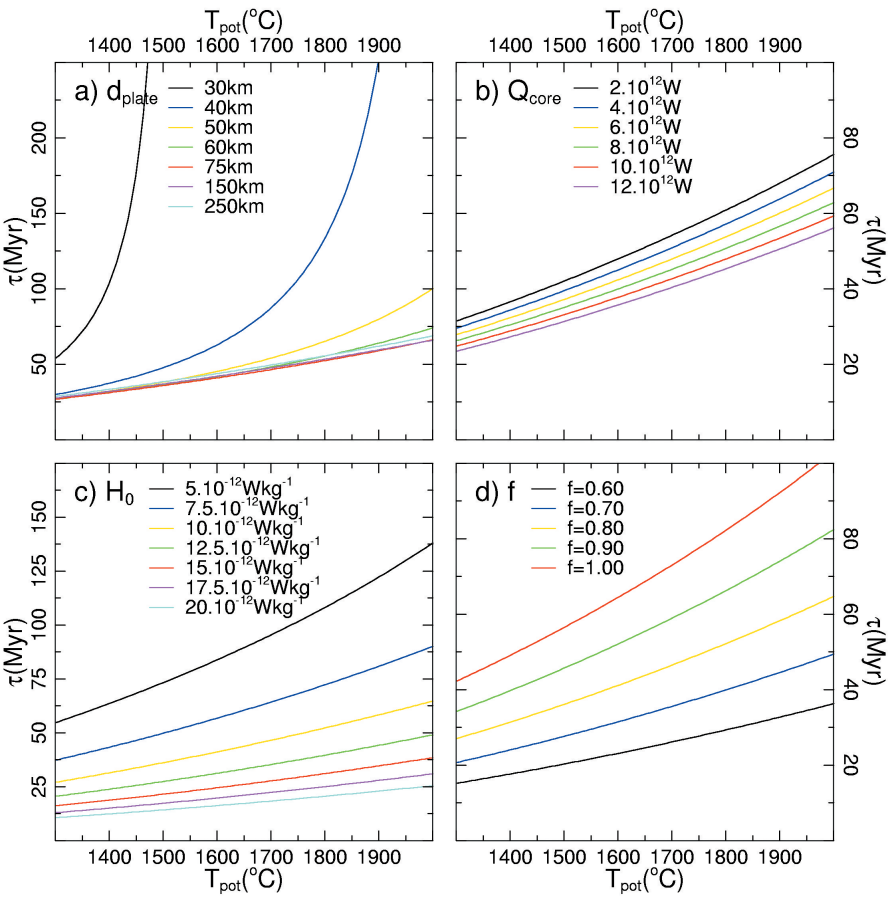

Figure 5.9: Sensitivity tests of the plate tectonics model to single parameters. Fixed values of the non-varying parameters are: Core heat flux $Q_{core} = 7\mathrm{TW}$, plate thickness $d_{plate} = 100\mathrm{km}$, internal heat productivity $H_0 = 10 \cdot 10^{-12}\mathrm{Wkg}^{-1}$, oceanic surface fraction $f = 0.80$, mantle cooling rate $-\frac{dT_{pot}}{dt} = 100\mathrm{KGyr}^{-1}$. The curves show the turnover time τ as a function of a) plate thickness d_{plate}; b) core heat flux Q_{core}; c) internal heat productivity H_0; d) extent of the active area f.

for the present situation and for a case representing the early Earth (4 Ga) and for two different values for the core heat flux, 3.5 TW and 10 TW. The timings are based on the rate of internal heating ($4.8 \cdot 10^{-12}\mathrm{Wkg}^{-1}$ for the present and $14.4 \cdot 10^{-12}\mathrm{Wkg}^{-1}$ for the early Earth) and the (estimated) extent of the continents ($f = 0.63$ for the present and $f = 0.97$ for the early Earth, McCulloch and Bennett, 1994). All four frames show the

potential temperature of the mantle on the horizontal axis, and the mantle cooling rate on the vertical axis (in K/Gyr). The contours indicate the turnover time τ that is required to maintain a cooling rate at a potential temperature corresponding to the position in the diagram. The shaded area indicates the region occupied by the exponential cooling histories shown in Figure 5.6, with the present-day Earth plotting near the left hand vertical boundary of this region. Note that Figure 5.8a,b and c,d are two sets of sections through two 3-D boxes, in which the internal heating rate is plotted on the third axis. In such a 3-D representation, it is possible to track any cooling history independent of the internal heating rate, whereas in 2-D sections such as those of Figure 5.8a,b and c,d (and also other figures below), any cooling history tracked in an individual frame is for a fixed internal heating rate. Because such a 3-D representation is difficult to bring across in 2-D figures, we use the 2-D sections and keep this caveat in mind. The core heat fluxes represent the range of values found in the literature as discussed in section 5.2.3.

From these diagrams we observe that for a fixed cooling rate, a longer turnover time is required at higher mantle potential temperatures. This is a result of the decreased plate thickness at higher potential temperatures, which causes an increase in the conductive surface heat flow and therefore reduces the convective heat flow that is required to maintain the specified cooling rate. For a constant mantle potential temperature, obviously, higher cooling rates require a shorter turnover time. Each figure shows a region in the lower right hand side corner where required turnover times are more than 500 million years (which is the maximum contour plotted). In these regions heat conduction through a static lithosphere is essentially sufficient to generate the required rate of cooling. This is a combined effect of the low cooling rates that characterize this regime which is effectively a stagnant lid situation (Solomatov and Moresi, 1996) and a thin lithosphere which is the result of a high mantle potential temperature.

The range of turnover times allowed by our model results for the present-day Earth, assuming an exponential cooling model, is indicated in Figure 5.8a-b by the left hand vertical boundary of the shaded area that envelopes the exponential cooling curves of Figure 5.6. Turnover times of about 30 to about 90 million years are permissible, consistent with the average age of subducting lithosphere on the present-day Earth of about 70 million years (Juteau and Maury, 1999, Table 11.1). For the early Earth, results consistent with exponential cooling indicate turnover times of about 40-50 million years (right hand side boundary of shaded area in Figure 5.8c-d). The effect of an increased core heat flux is that the surface heat flux must also increase in order to obtain the same specified cooling rate.

5.3.3 Sensitivity of plate tectonics results to the model parameters

Figure 5.9 shows the sensitivity of the results of the previous section to changes in plate thickness, core heat flux, internal heating rate and extent of the oceanic domain. In the experiments which produced these curves, all parameters were fixed (including the plate thickness, which in the previous experiments was a function of potential temperature following equation (5.18), see figure caption for values), except for the single parameter under investigation. In descending order of sensitivity, plate thickness, internal heating

rate, oceanic surface fractionional area and core heat flux influence the turnover time τ. There appears to be a threshold value for the importance of plate thickness. As Figure 5.9a shows, for thicknesses of more than 60 km, the effect of changing the thickness is minimal in the potential temperature range investigated. Below 60 km thickness, however, the turnover time increases strongly at higher temperatures. This effect is stronger for a thinner plate. It is caused by thermal conduction through the lithosphere taking over from conductive cooling of the lithosphere itself as the most important cooling factor. Note that the threshold thickness will be different for different cooling rates. The other parameters, core heat flux, internal heating rate and extent of the oceanic domain, have a more straightforward and linear effect, essentially scaling the turnover time more or less independent of the potential temperature (see Figures 5.9b,c,d).

5.3.4 Plate tectonics on Mars and Venus

The plate tectonics model of section 5.2.1 was also applied to Mars and Venus. The parameters that were adjusted to modify the model for these planets are the core and planetary radius (resulting in a different mantle heat capacity and surface to volume ratio), the surface temperature (controlling the surface heat flow), the average mantle density (controlling the mantle heat capacity), the core heat flux and the conversion factor between potential and volume averaged temperatures (resulting from different planetary radius and gravitational acceleration, which cause different adiabatic temperature profiles), using values listed in Table 5.2. Continents are assumed to be absent, so the oceanic surface fraction f is set to 1. The results of these experiments are shown in Figure 5.10. Two different values for the internal heating rate were used, which we assume to represent the present ($H_0 = 4.80 \cdot 10^{-12} W kg^{-1}$) and early ($H_0 = 14.40 \cdot 10^{-12} W kg^{-1}$) states of the planets. Again, the range of reasonable exponential cooling curves of Figure 5.6 is included as the shaded area. For present Mars, shown in Figure 5.10a, the results indicate that only extremely high cooling rates of more than 250 Kelvin per billion years requires the operation of plate tectonics. For lower, more likely cooling rates, turnover times are well over 500 million years, which essentially means that conductive cooling is sufficient. This is a result of the fact that, compared to the Earth, surface to volume ratio ($\sim R^2/R^3$) is relatively large. This results in conductive cooling through a comparatively greater surface area (scaling with R^2, see equation (5.13)) of a comparatively smaller heat reservoir (equation (5.2), scaling with R^3), which is more efficient. The same goes for early Mars (characterized in our model by an increased internal heating rate $H_0 = 14.40 \cdot 10^{-12} W kg^{-1}$), shown in Figure 5.10b, where the position of the planet may be expected in the right hand side half of the frame due to a higher mantle temperature. Venus, shown in Figure 5.10c-d (present and early), shows more Earth-like characteristics (see Table 5.2). At a probable present potential temperature similar to that of the Earth of $1300^o C$ with an upper limit of $1500^o C$ (Nimmo and McKenzie, 1998), turnover times for hypothetical plate tectonics would be on the order of tens to some hundreds of million years if we assume an exponential cooling scenario. A more likely scenario in which short episodes of rapid cooling (see Figure 5.7) and longer episodes of stagnation alternate would require turnover times of only some tens of million years or less (upper left of

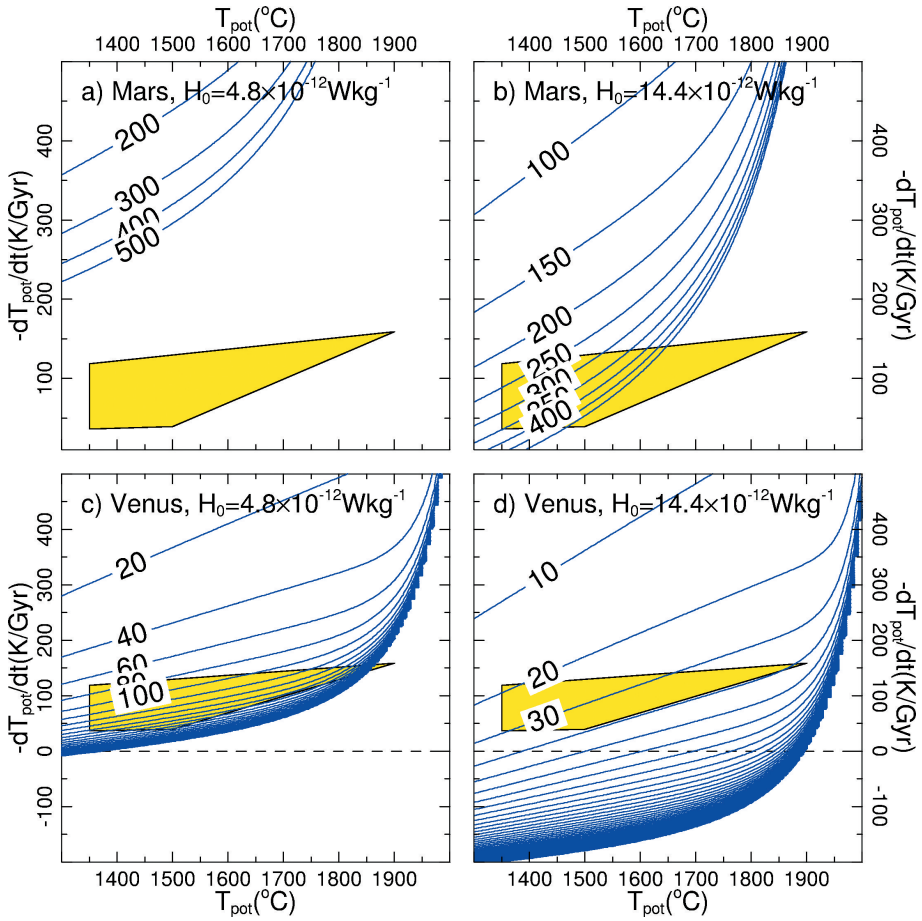

Figure 5.10: Turnover time τ for Mars and Venus for models with internal heating rates of $4.80\mathrm{Wkg}^{-1}$ and $14.40\mathrm{Wkg}^{-1}$. For other model parameters, see Table 5.2. For an explanation of the figure see caption of Figure 5.8.

Figure 5.10c) in the cooling episodes and (many) hundreds of million years (lower left of this frame) during the stagnation periods. For early Venus, some cooling mechanism other than conduction definitely seems required (see Figure 5.10d). If plate tectonics were this mechanism, turnover times on the order of some tens of million years are required, comparable to the results for the early Earth (Figure 5.8c-d). Note that we have included negative values for the cooling rate, since Venus may be heating up at the moment (Nimmo, 2002) and may have had more heating episodes (Turcotte, 1995).

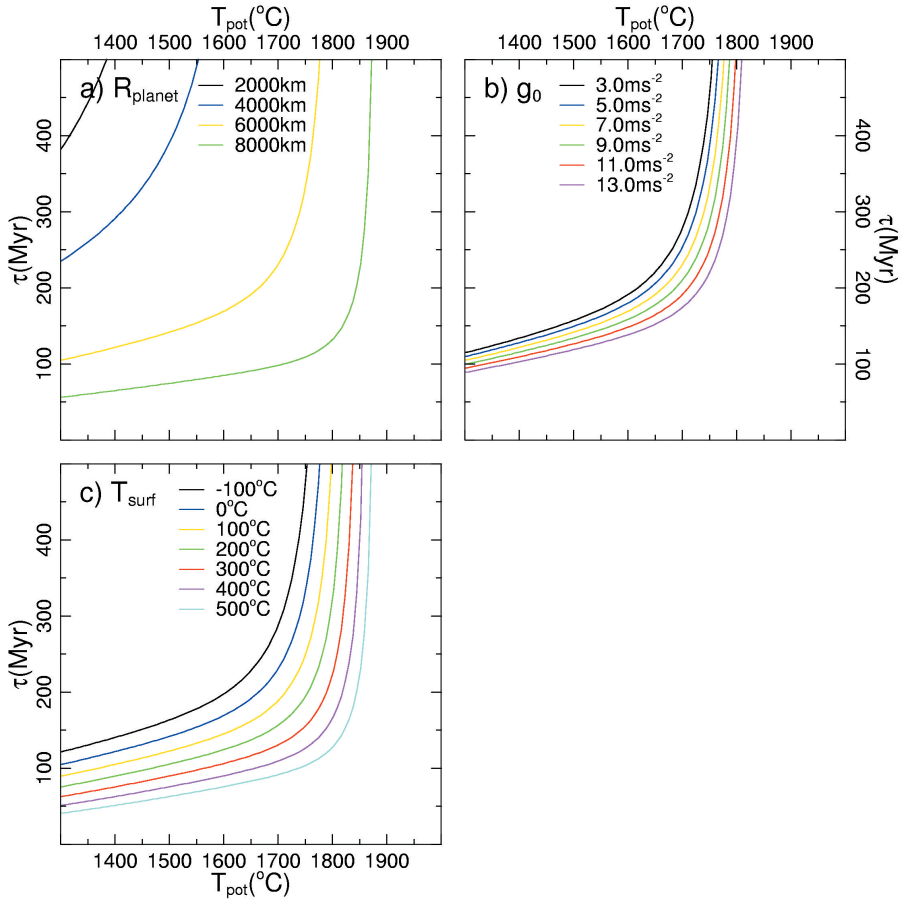

Figure 5.11: Variation of the turnover time τ as a function of (a) planet size R_{planet}, (b) gravitational acceleration g_0 and (c) surface temperature T_0. Values of non-varying parameters are $Q_{core} = 1\mathrm{TW}$, $d_{lith} = 100\mathrm{km}$, $H_0 = 4.8 \cdot 10^{-12}\mathrm{Wkg}^{-1}$, $f = 0.80$, $-dT_{pot}/dt = 100\mathrm{KGyr}^{-1}$, $g_0 = 7.0\mathrm{ms}^{-2}$, $R = 6000\mathrm{km}$. The core radius is half of the planetary radius in all cases. The potential to average temperature scaling factor $f_{T_{avg}}$ in equation (5.5) is recomputed for all different combinations of planet size and gravitational acceleration used.

5.3.5 Effects of planetary parameters on heat transfer by plate tectonics

In order to evaluate the effect of the different distinguishing parameters of the terrestrial planets separately, we have calculated the turnover time while varying one parameter (planetary radius, gravity or surface temperature) and keeping the others fixed. The results are shown in Figure 5.11a-c for these three parameters, respectively, for a fixed cooling rate of $100KGyr^{-1}$ (other parameters see figure caption). It is clear from this figure that the planet's size, through the surface area to volume ratio ($\sim R^2/R^3$), dominates the cooling behaviour of a planet, to such an extent that small planets can cool conductively at considerable rates, whereas larger planets need a more efficient cooling agent like plate tectonics to get a moderate cooling rate less than $100KGyr^{-1}$. The gravitational acceleration affects the adiabatic gradient ($\alpha gT/c_p$), but this effect is relatively minor. An elevated surface temperature tends to reduce the conductive heat flow, and therefore faster plate tectonics, if present, is required to maintain a certain rate of cooling.

5.3.6 Extrusion mechanism on Earth

Figure 5.12 shows the results of the extrusion models. It is similar to Figure 5.8 but it shows different quantities, the extrusion rate δ (black contours) in mMyr^{-1} and the global volumetric extrusion rate (red contours) in $\mathrm{km}^3\mathrm{yr}^{-1}$. The extrusion rate δ represents the global ($f = 1.0$) avarage thickness of basaltic crust produced in one million years. We consider this mechanism to operate globally (in contrast with plate tectonics), since continental flood volcanism is not uncommon. The extrusion rate δ and the global volumetric extrusion rate only differ by a factor of (surface area / 1 Myr). Again, four cases are investigated, using internal heating and continent extent values for the present ($H_0 = 4.80 \cdot 10^{-12}\mathrm{Wkg}^{-1}$) and early (4 Ga, $H_0 = 14.40 \cdot 10^{-12}\mathrm{Wkg}^{-1}$) Earth and two values for the core heat flux of 3.5 and 10 TW. The general trends are (1) a higher potential temperature reduces the lithosphere thickness and increases the temperature contrast over the lithosphere, thus increasing the conductive heat flux and decreasing the extrusion rate, (2) a higher cooling rate requires a greater extrusion rate, and (3) an increase in the internal heating rate (either radiogenic or from the core) requires an increase in the extrusion rate. For comparison, a rough estimate for the 'extrusion rate' of the present-day Earth is $\sim 70km^3yr^{-1}$ (100,000 km of ridges spreading at an average 2x5 cm/yr producing a crust of 7 km), which is somewhat less but of comparable magnitude to the numbers presented in Figure 5.12a,b (the left hand side boundary of the shaded area), although the mechanism is different. It is clear from Figure 5.12c and d that in the early Earth, conductive cooling through the lithosphere was sufficiently efficient above potential temperatures of approximately 1800^oC in the exponential cooling cases, indicated by the shaded area, to generate cooling without requiring magmatic processes, since the required extrusion rate δ is below 0 here. For lower potential temperatures, global volumetric extrusion rates are up to an order of magnitude higher than for the present-day Earth, less than 500 km^3yr^{-1}.

5.3.7 Sensitivity of the extrusion mechanism heat transfer

The sensitivity of the extrusion rate δ to the lithosphere thickness (a), core heat flux (b), internal heating rate (c) and extent of the 'oceanic' domain (d) is shown in Figure 5.13. Strong effects can be seen for the lithosphere thickness, where sufficiently low values may result in completely conductive cooling (no extrusion required), and the internal heating rate. The effect of surface area (assuming that the extrusion mechanism is active on only a part of the planet's surface) is smaller, and that of the core heat flux is quite limited in the parameter range that was investigated.

5.3.8 Extrusion mechanism on Mars and Venus

Figure 5.14 shows the results of the extrusion model for Mars and Venus, for internal heating values assumed to represent the recent and early history, respectively, of these planets. The results for present day Mars (Figure 5.14a) at the estimated present location of Mars in $T_{pot}, dT/dt$-space in the lower left hand side corner of the diagram indicate that only very limited volumetric extrusion rates are required for the cooling of Mars. Compared to Earth, the global volumetric extrusion rates are an order of magnitude smaller. In terms of extrusion rate δ, the difference is not as large due to the smaller surface area of Mars. Early Mars (Figure 5.14b) also requires only a small global volumetric extrusion rate, even for very high cooling rates, due to a combination of thinner lithosphere compared to present-day Mars and large surface area to volume ratio compared to larger planets. Things are quite different for Venus (Figure 5.14c,d). When assuming an exponential time dependence of planetary cooling as indicated by the shaded area, which may not be correct for Venus, we see volumetric extrusion rates on the order of 200-350 km^3yr^{-1}, up to 5 times greater than the present-day Earth's plate tectonics crustal production rate, and comparable to the rate that would be required for the present-day Earth if the extrusion mechanism were the main cooling agent (see Figure 5.12a,b). Early Venus also shows model results similar to those of the early Earth (see Figure 5.12c,d consistent with the similarity of the model parameters for both planets). Note that we have again included negative values for the cooling rate to show the effect of possible periods of heating in the planet's history.

5.3.9 Effects of planetary parameters on the extrusion mechanism heat transfer

For the extrusion mechanism, the sensitivity for planetary parameters is also investigated. The presentation of the results is similar to that of the plate tectonics sensitivity tests of Figure 5.15, and the parameter values are the same. The results show that both the planetary size (using a fixed value for g_0, which is rather artificial but the alternative would be to assume a relation between radius and gravitational acceleration, which is also artificial because of the dependence on composition) and the surface temperature may strongly affect the extrusion rate required for a prescribed cooling rate. The former

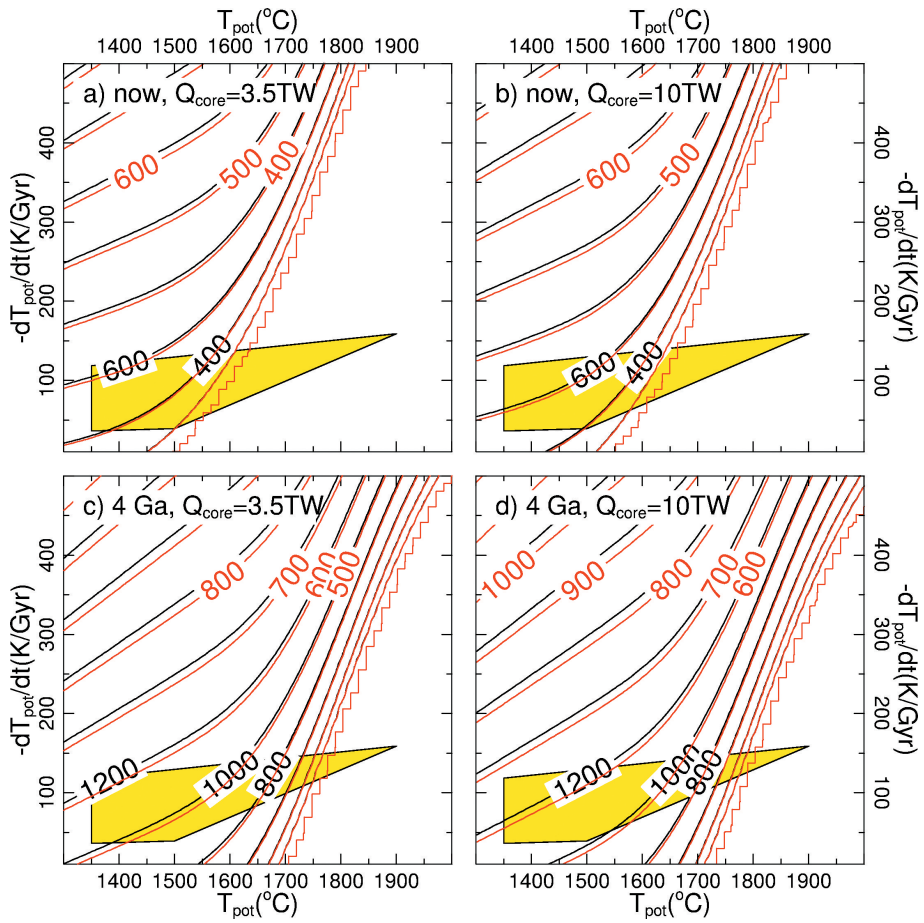

Figure 5.12: Results of the extrusion model for a core heat fluxes of 3.5 and 10 TW for the present and early Earth (in terms of radiogenic heat production rate and extent of the continents). Black contours indicate the extrusion rate δ in mMyr^{-1}, representing the average thickness of basaltic crust produced per million years for the entire planetary surface. Red contours indicate the global volumetric basalt production rate, in $\mathrm{km}^3\mathrm{yr}^{-1}$.

affects the planetary cooling efficiency through the surface area to volume ratio, and the latter is a factor in the temperature gradient over the lithosphere, determining the conductive heat transport. The gravitational acceleration, affecting the adiabatic gradient, has a limited effect, but obviously R_{planet} and g_0 are coupled quantities.

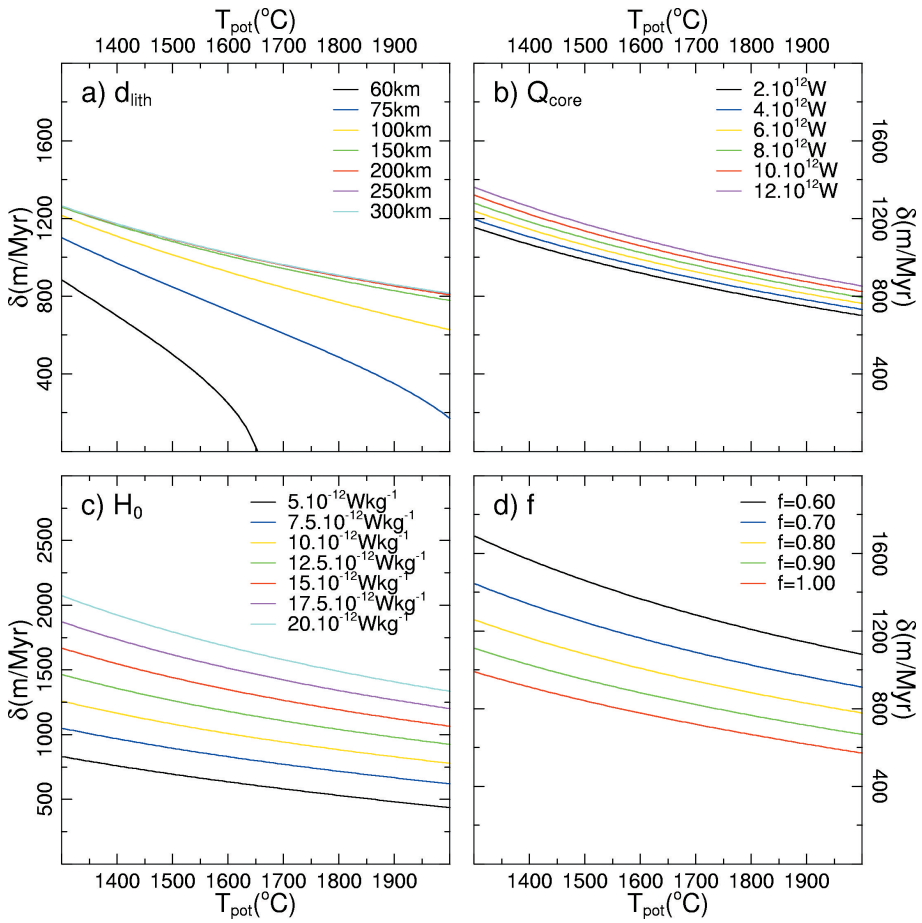

Figure 5.13: Sensitivity tests of the extrusion model to single parameters. Fixed values of the non-varying parameters are: Core heat flux $Q_{core} = 7\mathrm{TW}$, lithosphere thickness $d_{lith} = 150\mathrm{km}$, internal heat productivity $H_0 = 10 \cdot 10^{-12}\mathrm{Wkg}^{-1}$, oceanic surface fraction $f = 0.80$, mantle cooling rate $-\frac{dT_{pot}}{dt} = 100\mathrm{KGyr}^{-1}$. The curves show the extrusion rate δ as a function of a) lithosphere thickness d_{lith}; b) core heat flux Q_{core}; c) internal heat productivity H_0; d) extent of the active area f.

5.4 Discussion

5.4.1 Plate tectonics on the early Earth

Many speculations about the nature of plate tectonics in a hotter Earth have been presented. They often involve faster spreading than in the present situation (e.g. Bickle, 1978, 1986) or a longer mid-ocean ridge system (e.g. Hargraves, 1986), to transport a greater heat flux from the mantle. Our results, however, show that the hotter mantle itself generates the most important means of removing the increased heat flux from the mantle by thinning the lithosphere relative to a cooler mantle and thus significantly increasing the conductive heat flow though the lithosphere. This effect has also been noticed by Bickle (1978). If we compare the slope of the exponential model cooling curves of Figure 5.6 in T_{pot}, $\frac{dT_{pot}}{dt}$-space (indicated in Figure 5.8a-d by the shaded area) to the slope of the contours of equal turnover times, we observe that in all four models (Figure 5.8a-d) the turnover time required for a certain cooling rate increases faster with potential temperature than the actual cooling rate predicted by the exponential cooling model for higher mantle temperatures. In other words, the exponental cooling curves predict a *slower* rate of operation for plate tectonics rather than a faster at higher mantle temperatures. This is consistent with the argument of Hargraves (1986), who predicts slower plate tectonics on the basis of reduced slab pull and ridge push forces in a hotter mantle. Only when cooling pulses at much higher cooling rate (see Figure 5.7) than the exponential curve of Figure 5.6 are considered will the turnover time τ be reduced to lower values at higher mantle temperatures during these periods of increased cooling. However, in between these pulses, the turnover time will be significantly larger than in the exponential cooling case. As we only have a rough idea of the cooling history of the Earth, it is difficult to place the different geological eras in the diagrams produced in this work. Several authors have shown that plate tectonics becomes increasingly more difficult in a hotter Earth (Sleep and Windley, 1982; Vlaar, 1986; Vlaar and Van den Berg, 1991; Davies, 1992; Van Thienen et al., 2003c, chapter 4) on the basis of lithospheric buoyancy, which may limit the applicability of our plate tectonics results on the high end of the T_{pot} spectrum.

5.4.2 Extrusion mechanism on the early Earth

The volumetric extrusion rates found in our models can be compared to extrusion rates representative of processes similar to the extrusion mechanism in the more recent Earth, like hotspots and flood volcanism. Hotspots typically have basalt production rates of 0.02 to 0.04 km^3yr^{-1}. Phanerozoic flood volcanism may have eruption rates two orders of magnitude higher, about 0.75 to more than 1.5 km^3yr^{-1} (Richards et al., 1989), with peak rates possibly up to 10 km^3yr^{-1} (White and McKenzie, 1995). These numbers are still significantly smaller than the volumetric production rates up to $x \cdot 100km^3yr^{-1}$ found in Figure 5.12.

This means that if the mechanism played an important role in the cooling of the early Earth, much more extensive hotspot and flood volcanism activity may have been required to have sufficient cooling capacity. Much evidence is found for Archean and Proterozoic

duration (Myr)	area (km^2)	eruption rate $(\mathrm{km}^3\mathrm{yr}^{-1})$ d = 1 km	eruption rate $(\mathrm{km}^3\mathrm{yr}^{-1})$ d = 3 km	eruption rate $(\mathrm{km}^3\mathrm{yr}^{-1})$ d = 5 km
2409-2413	$7.42 \cdot 10^7$	18.6	55.7	92.8
2433-2451	$1.51 \cdot 10^8$	8.39	25.2	41.9
2582-2610	$7.37 \cdot 10^7$	2.63	7.90	13.2
2899-2903	$3.71 \cdot 10^7$	9.26	27.8	46.3

Table 5.4: Estimates of eruption rates for three different assumed flood basalt thicknesses d, based on areal extent estimates of superplume events by (Abbott and Isley, 2002, Table 8). The average of the mimimum and maximum areal extent reported by Abbott and Isley (2002) has been listed and used in calculating the eruption rates. The lowest two estimates for the average flood basalt thickness (1 and 3 km) are consistent with estimates of surface area and volume of several Phanerozoic flood basalts, listed in Table 1 of White and McKenzie (1995). We speculate that the higher value (5 km) may be more representative of larger scale events in the Archean.

flood volcanism. Arndt (1999) discusses many occurences all over the world. Abbott and Isley (2002) have identified a total of 62 superplume events and eras from the mid Archean to the present on the basis of flood basalts, dike swarms, high Mg rocks and layered intrusions, though especially for the Archean this is probably a lower limit because of preservation issues and lack of data. Using maximum dike widths and flood basalt surface area, they estimate the original extent of the flood basalts generated by the separate events. They find that both the magnitude and the frequency of these events was significantly higher during the late Archean and has declined since then. Abbott and Isley (2002) also identify six major events of which the estimated eruption volume of each was sufficient to cover at least 14-18% of the Earth's surface. When making an assumption about the average thickness of a flood basalt province, volumes can be computed and using estimated eruption times, volumetric eruption rates. In Table 5.4, estimates of eruption rates for four selected late Archean to early Proterozoic superplume events from Abbott and Isley (2002) have been calculated, using estimates for the average flood basalt thickness from Phanerozoic flood basalts (1-3 km, see Table 1 of White and McKenzie, 1995). The resulting numbers are of the same magnitude to up to one order of magnitude smaller than the eruption rates dictated by Figure 5.12c-d (lower middle to right corner for moderate cooling rates at Archean mantle temperatures). However, if we extrapolate further back to the early/middle Archean, we may expect volumetric extrusion rates to be even higher for these events, and the number of up to about $550 km^3 yr^{-1}$ required by Figure 5.12c-d for significant cooling rates is feasable with only a small number of active flood basalt provinces (last column of Table 5.4) for an early Earth that is only 150 Kelvin hotter than the present-day Earth (lower right corner of the shaded area in Figure 5.12c,d).

For higher temperatures during the early history of the Earth, the required extrusion rate is smaller and therefore the required amount and activity of flood volcanism is smaller

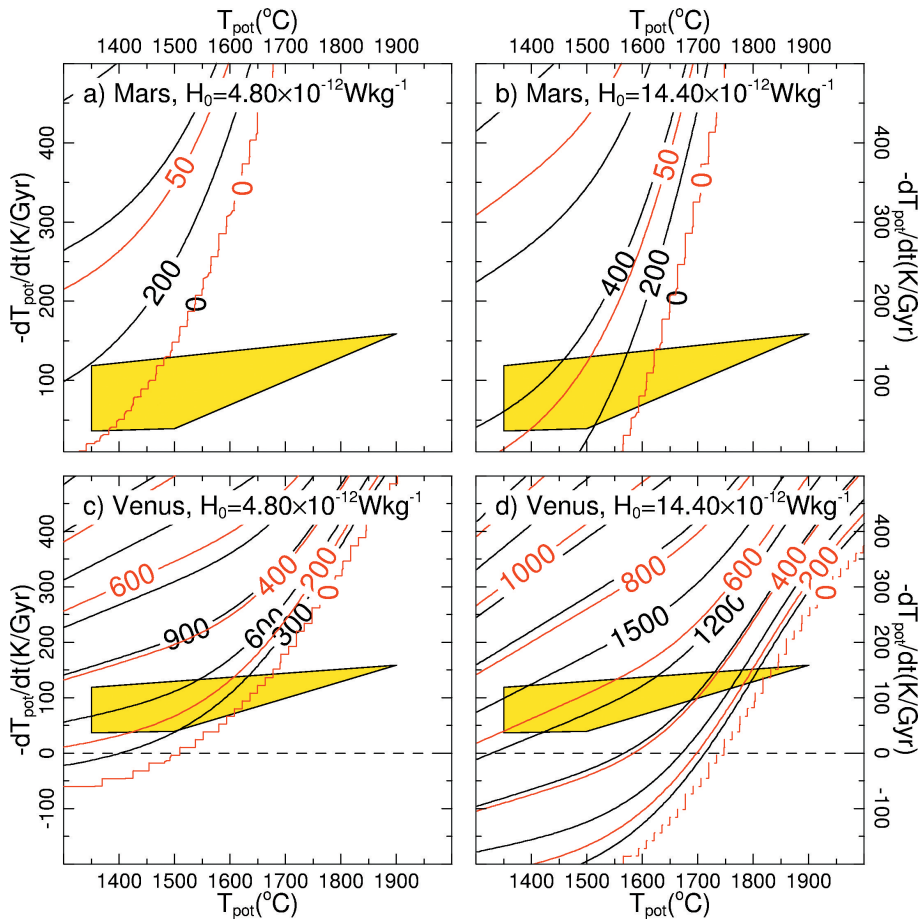

Figure 5.14: Results of the extrusion model for Mars and Venus, using two different values for the internal heating rate representing the recent and early histories of the planets. Black contours indicate the extrusion rate δ in mMyr^{-1}, representing the average thickness of basaltic crust produced per million years for the entire planetary surface area. Red contours indicate the global volumetric basalt production rate, in $\mathrm{km}^3\mathrm{yr}^{-1}$.

as well. For a hotter early Earth, say above 1750^oC, the numbers of Table 5.4 are similar to those in Figure 5.12 and a single flood volcanism province may be sufficient, combined with global conductive cooling, to attain significant mantle cooling rates.

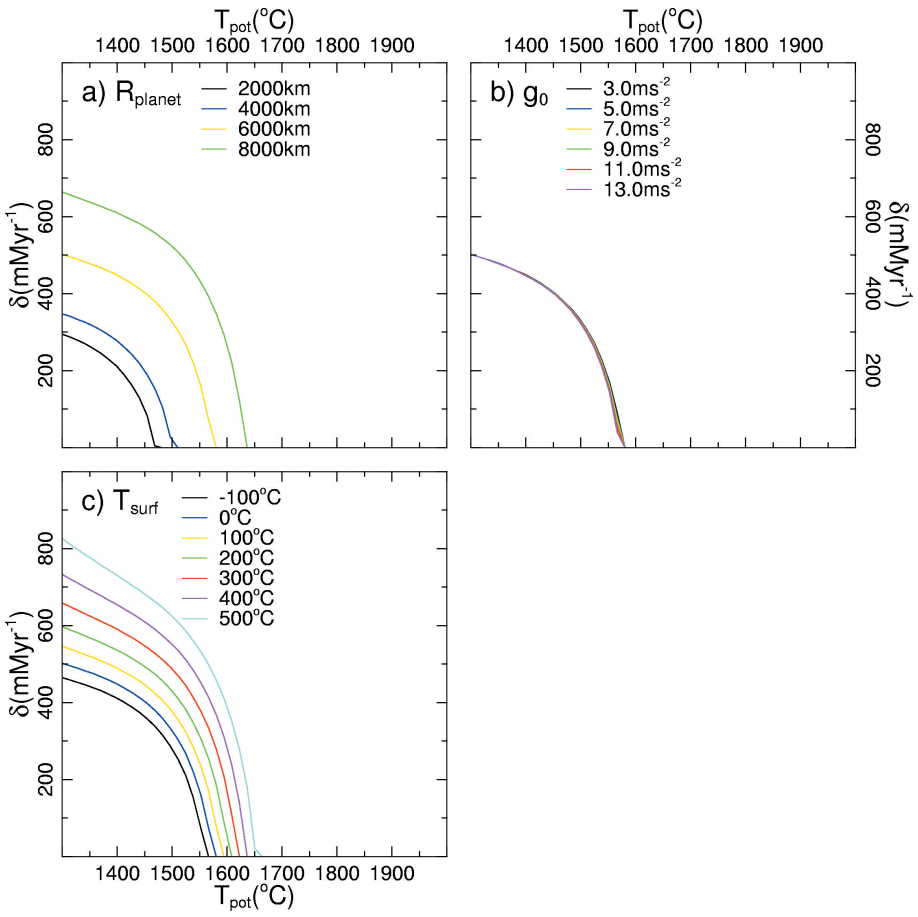

Figure 5.15: Variation of the extrusion rate δ as a function of (a) planet size R_{planet}, (b) gravitational acceleration g_0 and (c) surface temperature T_0. Values of non-varying parameters are $Q_{core} = 1\text{TW}$, $d_{lith} = 100\text{km}$, $H_0 = 4.8 \cdot 10^{-12}\text{Wkg}^{-1}$, $f = 0.80$, $-dT_{pot}/dt = 100\text{KGyr}^{-1}$, $g_0 = 7.0\text{ms}^{-2}$, $R = 6000\text{km}$. The core radius is half of the planetary radius in all cases. The potential to average temperature scaling factor $f_{T_{avg}}$ in equation (5.5) is recomputed for all different combinations of planet size and gravitational acceleration used.

5.4.3 Cooling mechanisms of Mars and Venus

The results, shown in Figure 5.10, clearly indicate that neither present nor early Mars requires plate tectonics to obtain considerable cooling rates on the order of 100 K/Gyr or more, and that the relatively small planet can cool conductively at considerable rates.

Nimmo and Stevenson (2000) suggest that plate tectonics or some other efficient cooling agent was active during the first 500 Myr of the history of Mars, in order to allow the core heat flow to rise above the conductive level and iniate core convection, which would produce a magnetic field of which the result is seen nowadays in the magnetisation of some ancient Martian crustal rocks (Acuña et al., 1999). During this initial phase, the model results of Nimmo and Stevenson (2000) show an average cooling rate of about 400 Kelvin per billion years, combined with a core heat flux of about 1.3 TW (using their 1450 km core size). Although our Mars models use a core heat flux of 0.4 TW, Figure 5.9 shows a low sensitivity of the results to variations in the core heat flux for Earth. For Mars, we expect the effect to be similarly small. Therefore, from the results of our model shown in Figures 5.10b and 5.14b (early Mars) at a cooling rate of $400\mathrm{KGyr}^{-1}$, we conclude that plate tectonics or basalt extrusion is not required to obtain this cooling rate at potential temperatures above $1700 - 1800^oC$, since conductive cooling through the lithosphere is able to sustain this cooling rate by itself. In other words, a significant contribution to the cooling of Mars by either plate tectonics or basalt extrusion is only to be expected when high cooling rates ($> 200\mathrm{KGyr}^{-1}$) take place in a relatively cool early Mars ($T_{pot} < 1700 - 1800^oC$). This appears to be in contradiction with earlier work of Reese et al. (1998). Earlier work based on buoyancy considerations of oceanic lithosphere already showed that plate tectonics is only possible on Mars when it has a low potential temperature below $1350 - 1400^oC$ (Van Thienen et al., 2003c, chapter 4). Our new results add evidence to the unlikelyness of plate tectonics on Mars during its history. Our models, however, do not take into account that in the reduced gravity of Mars, partial melting would generate a thick stratification of depleted, and therefore inherently less dense, mantle peridotite (Schott et al., 2001, 2002). This effect would possibly extend the thickness of the effective lithosphere, which we assume to coincide with our thermally defined lithosphere, to greater depths. This thickening of the lithosphere would decrease the required turnover time in the plate tectonics models, and increase the required volumetric eruption rate the extrusion models. Another effect that is not included in the calculations is that the use of a temperature and pressure dependent thermal conductivity rather than a constant value may significantly reduce the efficiency of conductive cooling through the lithosphere (Van den Berg and Yuen, 2002). There is plenty of evidence for an active volcanic history of Mars, the most important of which is the Tharsis region with its immense volcanoes. It is magmatic/volcanic of origin, and measures about $3 \cdot 10^8\mathrm{km}^3$ of material (Zuber, 2001). Most volcanic and magmatic activity took place during the Noachian and Hesperian (Dohm and Tanaka, 1999), spanning a period from 4.57 Ga to an estimated 2.9 Ga (Hartmann and Neukum, 2001). The minimum volumetric eruption rate is obtained from the ratio of the volume and maximum formation time, which is less than $0.2\mathrm{km}^3\mathrm{yr}^{-1}$. Since the system was possibly active for a shorter time, average eruption rates may have been higher, but the values probably remain low compared to for example the present day eruption rate at mid-ocean ridges of about $70\mathrm{km}^3\mathrm{yr}^{-1}$ (see above). Therefore, the magmatic activity involved in the formation of the Tharsis region probably did not have a strong effect on the cooling of Mars.

For Venus, the story is entirely different. The results for present Venus for both mechanisms (Figures 5.10c and 5.14c) show for the present estimated potential temperature

of about $1300 - 1500^oC$ (Nimmo and McKenzie, 1998) that some activity is required from either plate tectonics or basalt extrusion even if *no cooling at all* takes place. This is consistent with earlier results of Reese et al. (1998). The apparent lack of volcanic and plate tectonic activity on the present Venus therefore indicates the position of the planet in the diagrams is below the horizontal axis, or that the planet is heating up. This has also been suggested by Nimmo (2002).

Space observation of Venus indicates that the planet underwent global resurfacing between 300 and 600 million years before present (Schaber et al., 1992). During this episode of increased activity of crustal formation, Venus can be expected to have been cooling. Such a successive cooling and heating of Venus may be cyclical. Turcotte (1993, 1995) suggested that Venus has a history of periodic plate tectonics. From our results, plate tectonics and flood volcanism appear equally valid mechanisms of crustal production and heat loss in the cooling part of these hypothetical cycles.

5.5 Conclusions

Our model results show that for a steadily (exponentially) cooling Earth, plate tectonics is capable of removing all the required heat at a plate tectonic rate comparable to or even lower than the current rate of operation. This is contrary to the notion that faster spreading would be required in a hotter Earth to be able to remove the extra heat (e.g. Bickle, 1978). However, whether or not plate tectonics could work under these conditions is another question, which is addressed elsewhere (Sleep and Windley, 1982; Vlaar, 1985; Vlaar and Van den Berg, 1991; Van Thienen et al., 2003c, chapter 4). In the early Earth, the extrusion mechanism was probably more important, as indicated by ubiquitous flood basalts in the Archean (Arndt, 1999). For this mechanism to be able to contribute a significant part to the cooling of the Earth at rates comparable to the present rate of cooling, eruption rates up to one to two orders of magnitude higher than for Phanerozoic flood basalts are required. However, this is consistent with the increase in both frequency and magnitude of flood volcanism towards the Archean (Abbott and Isley, 2002). Mars seems to be capable of cooling conductively through its lithosphere without either plate tectonics or flood volcanism at significant cooling rates, due to its small size and, as a consequence, large surface to volume ratio. Only in hypothetical episodes of rapid cooling ($> 200 KGyr^{-1}$) during the early history of Mars, some additional mechanism may have been active, which can be either plate tectonics or flood volcanism. We confirm the inference of Nimmo (2002) that the mantle of Venus is heating up. This suggests a cyclicity of heating and cooling, as suggested earlier by Turcotte (1993, 1995). Throughout its history, this planet has required a mechanism additional to conduction for the cooling of its interior (assuming that the presently elevated surface temperature is representative of the planetary history), operating at rates comparable to those of the Earth.